ELSEVIER

NMR methods in fragment screening: theory and a comparison with other biophysical techniques☆

Claudio Dalvit[1,2]

[1] Novartis Institute for Biomedical Research, CH 4002 Basel, Switzerland
[2] Department of Drug Discovery & Development, Italian Institute of Technology, 16163 Genova, Italy

Nuclear magnetic resonance, surface plasmon resonance and fluorescence spectroscopy (particularly fluorescence anisotropy and fluorescence lifetime) are techniques often applied to fragment screening. These methodologies are analyzed on the basis of their performance, strengths, limitations and pitfalls. NMR-based screening, despite its low intrinsic sensitivity, offers the largest dynamic range and is capable of capturing very weak interactions. Theoretical simulation demonstrates the power of some NMR experiments, in particular those with fluorine observation, in detecting protein interactions for fragments tested at concentrations orders of magnitude lower than their dissociation binding constants. This apparently counterintuitive finding enables the identification of hits that are insoluble at the concentrations required for detection by other biophysical techniques. However it is evident that several techniques should be applied and the data analyzed on the basis of their complementarities.

Introduction

During the past two decades, the identification of hits in the early stage of drug discovery has relied heavily on high-throughput screening (HTS) [1]. However, HTS has not always been fruitful, and there have been several drug discovery projects in which HTS has failed to deliver meaningful potential hits. Therefore, there is a constant need for alternative approaches to HTS to overcome these limitations. Fragment-based drug discovery (FBDD) offers a potential solution to the HTS limitations [2–8]. Screening molecular fragments, rather than drug-sized molecules, enables one to explore a dramatically larger portion of chemical structure space with considerably fewer compounds [9,10].

The field of FBDD has developed significantly over the past 10 years and is now recognized for its important contribution to the drug discovery process. The number of pharmaceutical and academic groups actively involved in fragment-based research has increased steadily and there have been noteworthy improvements in instrumentation and experimental design. Only a few years after the first applications, there are already several clinical and preclinical candidates for which there is a clear statement in the public domain that the candidate drugs were derived from fragment-based drug discovery approaches [2,3].

The crucial step in this drug discovery process is the reliable identification of the initial fragments (i.e. the 'molecular anchors' or 'minimal recognition motifs') that, despite their high ligand efficiency (LE) [11–14], interact only weakly with the receptor because of their small size.

A large variety of biophysical techniques have been applied in this initial phase of the FBDD process [5–8]. Three of the most popular methodologies are nuclear magnetic resonance (NMR), surface plasmon resonance (SPR) and fluorescence spectroscopy, in particular fluorescence anisotropy (FA) and fluorescence lifetime (FL). Many of the lead compounds in FBDD projects have originated from the initial fragments discovered with these biophysical tools applied to binding or biochemical assays. Although X-ray crystallography has also been used in the screening process of fragment libraries [5–7], its pivotal role is in the protein-bound structure determination of previously identified fragments.

Often two or more techniques are used simultaneously in this process for reliable identification of the chemical moieties. However, these biophysical techniques are subject to artifacts and

☆ The NMR methods applied to fragment screening are analyzed on a theoretical basis and a comparison of these methodologies with two other very popular biophysical techniques is presented.

E-mail address: claudio.dalvit@iit.it., claudiodalvit@hotmail.com

1359-6446/06/$ - see front matter doi:10.1016/j.drudis.2009.07.013

interferences that might lead to false-positive or false-negative results. Causes other than the desired one-to-one binding interaction are responsible for the false results.

This problem is particularly pronounced when screening fragments owing to the small free energy change originating from the interactions of the molecule with the receptor. For example, the difference in binding energy for a fragment interacting with the receptor with a dissociation binding constant (K_D) of 1 mM is only −4.09 kcal at 25 °C.

The type of artifacts and the detection threshold might vary among the different techniques so that a molecule resulting positive in one assay is not detected in another assay or vice versa. In our experience, not every fragment hit identified with NMR-based screening could be observed with other biophysical techniques, and the theoretical explanation for this discrepancy is described in this work. Crucial for the subsequent utilization of these fragments is their validation as *bona fide* binders. The X-ray structure of the fragment bound to the receptor provides final binding evidence and, in addition, it delivers the relevant structural information for initiating lead optimization via medicinal and/or combinatorial chemistry attempts. However, in practice, it is not always possible – because of different experimental causes – to observe electron density of fragment hits bound to their receptor. In these cases, a thorough understanding of the underlying theory of each screening methodology and the potential sources of artifacts can guide the scientist in the decision-making process on whether to pursue or discard these dubious but potentially very relevant NMR hits. It is the goal of this article to provide a comprehensive insight into the performance, the advantages and the limitations of NMR-based methodologies applied to FBDD and to compare them with SPR and the fluorescence-based techniques FA and FL. Table 1 provides an overview of the properties of the methodologies analyzed in this work and applied to fragment screening.

An apparently counterintuitive finding demonstrates that the often made statement that fragment screening needs to be performed at high concentration to detect weakly binding fragments does not apply to a class of NMR experiments, in particular to the fluorine-detected experiments. The detection of weak-affinity fragments in these NMR experiments is possible by screening the molecules at concentrations that are orders of magnitude smaller than their dissociation binding constant.

Surface plasmon resonance

SPR is a label-free technology for monitoring biomolecular interactions [15–19]. Some people argue that the term label-free often used is not properly correct because the protein is tethered to a surface via coupling chemistry. The technique is very attractive owing to its low protein consumption. The immobilization of the protein onto a chip surface enables up to thousands of molecules to be sequentially screened using the same surface before renewal of the protein is required.

The detected response in an SPR experiment corresponds to the change in the surface plasmon resonance angle (θ_{spr}) upon interaction of the fragment with the immobilized protein. The change is quantified in resonance units, or response units (RUs), with 1 RU equivalent to a shift of 10^{-4} degrees.

TABLE 1

Biophysical techniques frequently applied to fragment screening

Properties and requirements	NMR techniques						Fluorescence techniques		SPR
	Ligand detection				Protein detection				
	STD and WaterLOGSY	$^{H}R_2$	$^{F}R_2$	$^{H}R_{1,s}$	SAR by NMR		FA	FL	
Response dependence	[EL]	[EL]/[L_T]	[EL]/[L_T]	[EL]/[L_T]	[EL]/[E_T]		[EL]/[E_T]	[EL]/[E_T]	[EL]/[E_T]
Intrinsic sensitivity	Low	Low	Low	Low	Low		High	High	High
Dynamic range	Large	Large	Very large	Large	Medium-large		Small	Small	Small
Protein size sensitivity	↑	↑	↑	↑	↓		↑	[a]	↓
Fragment concentration	μM to mM	Low μM	Low μM	Low μM	μM to mM		μM to mM	μM to mM	μM to mM
Protein concentration	Low μM	Low μM	nM to low μM	Low μM	μM		nM	nM	μM to mM[b]
Volumes	30–500 μL						5–50 μl	5–50 μl	50–100 μl

The arrows ↑ and ↓ indicate, respectively, increase and decrease in performance by increasing the size of the protein.

[a] The change in the fluorescence lifetime upon binding to the protein is virtually unpredictable.

[b] Despite the high protein concentration used with SPR, the protein consumption is very low because the same protein-coated surface is used for sequentially screening the molecules.

The detected response, R, of a fragment interacting with the receptor is given by Eq. (1) [18]:

$$R = \frac{[L_T] \times R_{max}}{[L_T] + K_D} \quad (1)$$

where $[L_T]$ and K_D are, respectively, the concentration and dissociation binding constant of the fragment. R_{max} is the maximum response achievable when all the protein target is complexed with the tested molecule and is given by Eq. (2) [18] given below:

$$R_{max} = \frac{(\text{Immob. Target} \times \text{Target Activity} \times \text{MW Fragment})}{\text{MW Target}} \quad (2)$$

where Immob. Target is the value of RU observed upon immobilization of the protein, typically in the several thousands range; Target Activity is a factor ranging between 0 and 1 that accounts for the fraction of the immobilized protein molecules in the active form; and MW Fragment and MW Target are the molecular weights of the fragment and protein, respectively.

The response in SPR is proportional to the fraction of bound protein $[EL]/[E_T]$, where $[EL]$ and $[E_T]$ are the concentration of bound and of total protein, respectively.

Eq. (1) can be rearranged, resulting in Eq. (3) given below:

$$\frac{[L_T]}{K_D} = \frac{R}{(R_{max} - R)} \quad (3)$$

Typical detection cutoff value for R is ~5 RU, which is based on an average typical negative control signal plus 3 standard deviations [18]. Figure 1 shows a simulation of Eq. (3) displaying the minimum required ratio $[L_T]/K_D$ for binding detection as a function of the MW of the fragment and for two proteins of different size.

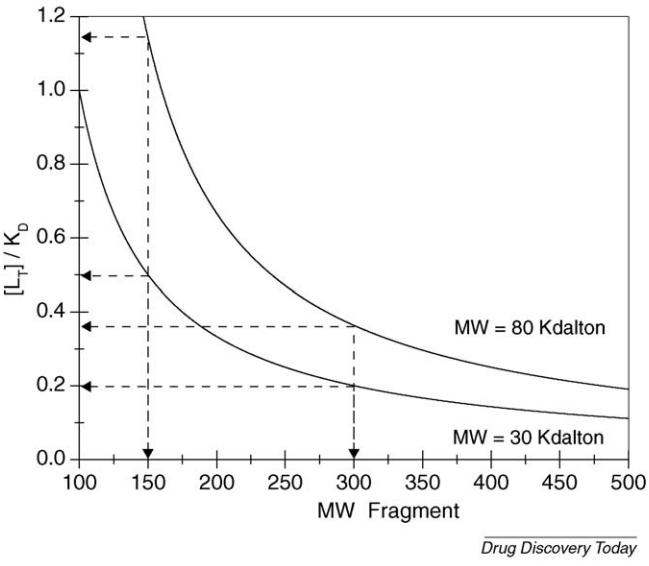

FIGURE 1

Fragment detection limit expressed as the ratio $[L_T]/K_D$ for protein binding in a typical SPR experiment as a function of the molecular weight of the fragment and for two proteins of different size, as indicated on the graph. The dashed lines are drawn at 150 and 300 Da, which correspond, respectively, to the low and high end of a fragment library. The simulation was performed with Eq. (3), where R_{max} was calculated from Eq. (2). An immobilization target value of 6000 for the protein of 30 kDa and 10 000 for the protein of 80 kDa, a Target Activity value of 0.5 and a detection cut-off value for R of ~5 RU were used as reported in the literature [18]. According to the graph, fragments are detected only if they are lying above the curves.

Two important issues emerge from the simulation of Figure 1. First, protein–fragment interactions can be detected only by working at fragment concentrations comparable to the K_D of the fragment. This is simply because of the limited dynamic range ($R_{max} - R$) of the experiment. Second, the dynamic range becomes smaller with increase in size of the protein investigated. Reduction in ($R_{max} - R$) is due to a reduction in the R_{max} resulting from a smaller MW Fragment/MW Target ratio in Eq. (2). According to the simulation of Figure 1, the detection of a fragment of MW = 150 is possible when $[L_T]$ is $> 0.5\ K_D$ for a protein of 30 kDa and $>1.14\ K_D$ for a protein of 80 kDa. These values become, respectively, $>0.2\ K_D$ and $>0.36\ K_D$ for a fragment of MW = 300. An improvement in the detection limits could be achieved by increasing the immobilization target level and with all the protein molecules in the active form (Target Activity ~1). However, immobilization levels larger than 15 000 RU are not normally possible [18]. In the perfect experimental condition with 100% of the protein in the active form, in practice never fulfilled, the detection limits become $[L_T] > 0.2\ K_D$ (MW = 150), $[L_T] > 0.09\ K_D$ (MW = 300) for the 30 kDa protein target and $[L_T] > 0.36\ K_D$ (MW = 150), $[L_T]$ is $> 0.15\ K_D$ (MW = 300) for the 80 kDa protein target. The high concentration required for the detection of the weak-affinity fragments limits the use of SPR to sufficiently soluble fragments. This weakness in the detection becomes a crucial issue when screening targets for which the fragments do not have a large binding efficiency index [13], such as those found among the inhibitors of protein–protein interactions.

When applicable, however, SPR is a content-rich method enabling the analysis of binding kinetics, thus providing the association rate constant, k_{on}, and dissociation rate constant, k_{off}, of the interactions [20]. The possibility of determining in one experiment K_D, k_{on} and k_{off} allows the ranking of the fragments according to these three physical properties. Different studies have shown that significant differences in k_{on} and k_{off} can be observed for ligands with similar K_D that the k_{on} and k_{off} are not correlated to each other, and that the k_{on} and k_{off} are related to the structural features of the ligands [20,21].

Fluorescence anisotropy and fluorescence lifetime

FA and FL used in competition mode with a fluorophore-labelled reporter are very popular techniques for screening purposes because of the compact format of the assay and the high absolute sensitivity [22–24]. The methodologies can be used in binding or biochemical assays.

The setup of an FA assay requires first the chemical derivation of a known very high affinity ligand and subsequent covalent linking of a fluorescent dye with a suitable lifetime of the excited state τ_F.

When a fluorophore is excited with polarized light, the emitted light is also polarized. Rotational diffusion of a fluorophore results in depolarization of fluorescence.

Anisotropy (A), also referred to as r, is defined as [25]:

$$A = \frac{I_{//} - I_{\perp}}{I_{//} + 2I_{\perp}} \quad (4)$$

where $I_{//}$ and $I_{\perp}$ are the emission intensity parallel and perpendicular, respectively, to the plane of the excited light. Note that

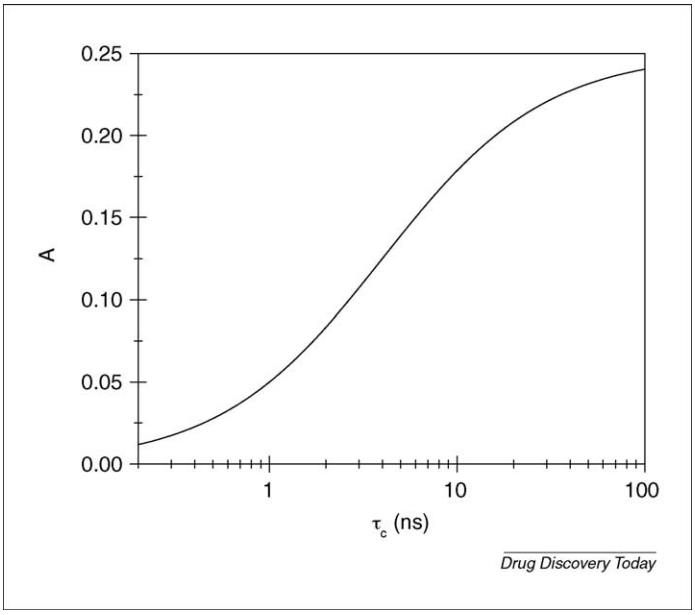

FIGURE 2

Simulation performed with Eq. (5) showing the behavior of the anisotropy (A) of the fluorescein-tagged reporter molecule (spy molecule) S as a function of the correlation time τ_c. The value for the limiting anisotropy A_0 was 0.25 and the fluorophore lifetime τ_F was 4 ns [22]. The *x* and *y* axes are on logarithmic and linear scale, respectively.

polarization (*P*) is interchangeable with anisotropy, according to the expression $P = 3A/(2+A)$. The anisotropy value depends on the fluorophore rotational correlation time τ_c and lifetime of the excited state τ_F, according to [22]:

$$A = \frac{A_0}{1 + (\tau_F/\tau_c)} \quad (5)$$

where A_0 is the limiting anisotropy that varies with wavelength and dye, and it is typically 0.25 for fluorescein, a frequently used fluorophore.

A simulation of the behavior of the anisotropy as a function of the correlation time, τ_c, for fluorescein is shown in Figure 2. The function is monotonic with τ_c and, therefore, can be used for studying protein–ligand interaction. The observed anisotropy, A_{obs}, of the fluorophore-labelled reporter molecule S (also known as spy molecule) interacting with the receptor is given by Eq. (6) [22]:

$$A_{obs} = \frac{\{A_f([S_T] - [ES]) + A_b Q[ES]\}}{([S_T] - [ES] + Q[ES])} \quad (6)$$

where A_f and A_b are the anisotropy of the fluorophore-free and bound to the receptor, respectively, and *Q* is the ratio of the respective quantum yields in the bound and free state ($Q = \Phi_b/\Phi_f$). In the simple approximation of $Q = 1$ (i.e. the fluorescent intensity is the same in the free and bound state), Eq. (6) simplifies to Eq. (7):

$$A_{obs} = A_f p_f + A_b p_b \quad (7)$$

The term p_b is the fraction of bound spy molecule defined as $p_b = [ES]/[S_T]$, and p_f is the fraction of free spy molecule defined as $p_f = 1 - [ES]/[S_T]$, where [ES] and $[S_T]$ are the concentration of protein complexed with the spy molecule and the total concentration of the spy molecule, respectively.

The observed anisotropy is, according to Eqs. (5) and (7), a weighted average of two values (bound and free) with comparable magnitude. This results, as is the case for the SPR technique, in a limited dynamic range (A_b–A_f), as can be appreciated from the simulation of Figure 2. The fluorophore attached to the spy molecule will have a longer τ_c than the fluorophore alone. This results in an increase of the anisotropy value of the free state. In addition, the fluorophore of the spy molecule in the bound state is often located on the surface of the protein, lest it interferes with the binding of the spy molecule to the receptor. In this situation, internal mobility of the fluorophore, also known as the 'propeller effect', can reduce the anisotropy of the bound state. These two phenomena significantly reduce the dynamic range. Therefore, the FA assay has to be performed under conditions of high fraction of bound fluorophore-tagged spy molecule $[ES]/[S_T]$ [23]. This requires a protein concentration that is larger than the spy molecule concentration and comparable to (or, better, larger than) the K_D value. A chemical fragment, L, binding to the receptor and competing with the spy molecule is detected only if a meaningful decrease in the anisotropy value of the spy molecule is observed or, in other words, if a large reduction of p_b is achieved. The same considerations apply to the FA-based functional assay.

The sensitivity of the method is directly proportional to $[EL]/[E_T]$. Therefore, similarly to SPR technique, protein–fragment interactions are monitored only by working at fragment concentrations comparable to the K_D of the fragment. Another weakness of FA is associated with the optical interferences originating from the tested molecule that can result in the generation of false-positives or false-negatives [26–28]. Insoluble compounds, aggregates, light absorption by compounds and intrinsic fluorescence of the fragments over the spectral range of the reporter fluorophore interfere with the measurements. It is evident that these interferences are more pronounced in fragment screening owing to the high concentration of the tested fragments. FL measurements have been added to FA assays to reduce the number of false-positives caused by aggregated compounds and identify some of the autofluorescent molecules [29–31]. However, the FL measurements performed with a suitable reporter (i.e. a spy molecule with $Q \neq 1$) also suffer from the limited dynamic range ($\tau_F^b - \tau_F^f$), where τ_F^b and τ_F^f are the reporter fluorescence lifetime of the excited state in the bound and free state, respectively. Therefore, the detection of the fragments, like in FA measurements, is achieved in a binding or biochemical assay only by testing the chemical scaffolds at concentrations comparable to their K_D. The properties and requirements in a FL assay are the same as those for a FA assay, as described in Table 1, with the exception of the protein size sensitivity. In contrast to the fluorescence anisotropy, the change in lifetime upon binding is virtually unpredictable.

When it comes down to the screening of large proprietary compound collections, FA and FL measurements are second to none. The high sensitivity of these techniques, their amenability to automation and the compact format of the assay enables rapid screening of several hundred thousands of separate compounds in the matter of only a few days.

Nuclear magnetic resonance

Among the three biophysical techniques discussed here, NMR is the method that has the lowest absolute sensitivity. A plethora of NMR methods have been proposed for fragment screening [32,33]. Some of these NMR experiments currently used are summarized in

Table 1, which also lists SPR, FA and FL for the sake of comparison. The methods are grouped according to the sensitivity dependence of the measured response.

Protein chemical shift perturbations

The response in the protein-based NMR screening experiments of which SAR by NMR is a representative [34,35] is, as in the SPR experiments, proportional to $[EL]/[E_T]$.

Eq. (1) can also be applied to protein-based NMR screening, where R_{max} now corresponds to $\Delta_{max} = (\delta_b - \delta_f)$ and R is $\Delta_{obs} = (\delta_{obs} - \delta_f)$. The terms δ_f, δ_b, δ_{obs} are the protein resonance chemical shifts, respectively, in the absence of the ligand, in the fully ligand-occupied state and in the assay conditions. However, because of the high protein concentration required by the experiments (typically in the order of 30 to 50 μM for the detection of the protein signals), the approximation $[L_T] = [L]$ (where [L] is the concentration of free ligand) used for deriving Eq. (1) is not always strictly correct. Therefore, a more appropriate expression describing the response in the protein-based NMR screening experiments is given by Eq. (8) [36,37]:

$$\Delta_{obs} = \Delta_{max}\left\{\frac{[E_T] + [L_T] + K_D - \sqrt{([E_T] + [L_T] + K_D)^2 - 4[E_T][L_T]}}{2[E_T]}\right\} \quad (8)$$

If the protein chemical shift difference between the bound and free state Δ_{max} is not large, it is necessary to achieve a large fraction of ligand-bound protein $[EL]/[E_T]$. This requires a high fragment concentration if the molecule has a very low-affinity for the receptor. This is not always possible, however, because of solubility limitations (as discussed above). In addition, the method for standard applications is restricted only to small-size and medium-size proteins. Screening with large proteins is also possible in some cases, but this requires extensive and expensive deuteration of the protein.

When compared to the other techniques discussed here, protein-based NMR screening represents the only method capable of providing information about the precise location of the interaction of the fragment on the protein. However, it is worth noting that chemical shift perturbation mapping with a ^{15}N-labelled protein can sometimes provide only an approximate binding location. Changes in protein dynamic upon ligand binding can result in pronounced shift perturbations even for amide resonances of amino acids located far away from the ligand-binding site. More reliable determination of the binding site is achieved with chemical shift perturbation mapping of ^{13}C-labelled proteins.

WaterLOGSY and STD

WaterLOGSY [38] and STD [39,40] experiments rely on intermolecular magnetization transfer via the bulk water and directly via the protein, respectively, for the detection of molecules interacting with the receptor. The STD effect and WaterLOGSY effect (defined as the difference of signal in the absence and presence of protein) are proportional to the concentration of bound ligand [EL], whereas the WaterLOGSY effect in the presence of only the protein is proportional to $A \times [EL] + B \times [L]$, where A and B are sums of cross-relaxation rates in the bound and free state, respectively. A large response is achieved in these experiments when increasing the term [EL], reaching the maximum value R_{max} for $[EL] = [E_T]$. However, owing to the large intermolecular and intramolecular dipole–dipole interactions in the bound state, the detection of fragments is possible even working at a concentration much lower than the K_D value. An example of this is the identification of a weak-affinity NMR hit via WaterLOGSY for the β-secretase receptor [41]. The fragment was identified by working at a ratio $[L_T]/K_D$ of only 0.07. This initial fragment was then developed through FBDD into a potent inhibitor [42].

A crucial issue of these experiments is their limited sensitivity, which restricts the size of compound libraries that can be tested. A recent pulse-sequence optimization of the original WaterLOGSY experiment has resulted in a sensitivity improvement, enabling a reduction of the measurement time [43]. Another weakness associated with these experiments is the possibility of detection of false-positives. Molecules that aggregate in solution will give a response in the WaterLOGSY and STD experiments similar to that in the presence of protein binding. However, NMR control experiments performed in the absence of protein and NMR competition binding experiments identify the false-positives.

Transverse and selective longitudinal relaxation rate experiments

The observed response R_{obs} in the ^{1}H, ^{19}F and ^{31}P transverse relaxation rate R_2 experiments for a fragment weakly interacting with the receptor is given by Eq. (9):

$$R_{obs} \approx R_f\, p_f + (R_b + R_{ex})\, p_b \quad (9)$$

where the R_f and R_b here correspond to the transverse relaxation rates in the free and bound state, p_f and p_b correspond to the fraction of free and bound fragment, respectively and R_{ex} is the exchange contribution deriving from the difference of the isotropic chemical shifts of the fragment resonance(s) in the bound and free state. The dynamic range $[(R_b + R_{ex}) - R_f]$ can be very large in these experiments, and its value increases with the size of the macromolecular target.

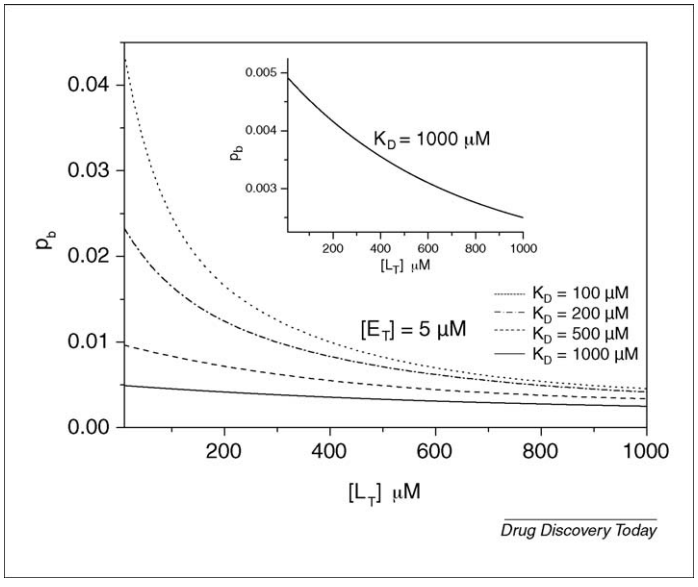

FIGURE 3

Simulation performed with Eq. (10) showing the fraction of protein-bound fragment p_b as a function of its concentration $[L_T]$ (range from 10 to 1000 μM) and for four different values of K_D as indicated on the graph. The protein concentration was 5 μM. The inset contains the vertically expanded region of the simulation performed with the K_D value of 1 mM.

Eq. (9) with $R_{ex} = 0$ applies also to the ^1H selective longitudinal relaxation rate $R_{1,s}$ experiments, where R_f and R_b are the selective longitudinal relaxation rates in the free and bound state, respectively. The sensitivity to ligand detection in the transverse and selective longitudinal experiments is proportional to the fraction of bound fragment p_b with $p_b = [EL]/[L_T]$. Proper setup of these experiments is crucial for the detection limit. These screening experiments can be recorded in a direct or competition mode. For comprehensive reviews of these methodologies, see Refs. [44–48].

The fraction of bound fragment is given by Eq. (10):

$$\frac{[EL]}{[L_T]} = \frac{[E_T] + [L_T] + K_D - \sqrt{([E_T] + [L_T] + K_D)^2 - 4[E_T][L_T]}}{2[L_T]} \quad (10)$$

Figure 3 shows a simulation of the fraction of bound fragment as a function of the fragment concentration $[L_T]$ and for four different dissociation binding constant values. According to the simulation, p_b increases as the fragment concentration decreases. This seems, at first, to be counterintuitive because very weak ligands can be detected only by working at concentrations that are orders of magnitude lower than their binding constant. Therefore, these NMR screening experiments should always be recorded at a very low fragment concentration compatible with the absolute sensitivity of the NMR instrument. A 10–30 μM fragment concentration is possible with a standard probe-head, whereas this value can be reduced to only a few μM with the use of cryogenically cooled probe-heads. The low fragment concentration used in the experiments is fundamental for the detection of weak fragments that are not soluble at concentration comparable to their K_D. These NMR hits are sometimes not detected with other biophysical techniques, and their structure bound to the receptor is not observed in X-ray studies because of their low solubility. The approach that is typically taken in these situations is to stop all activities with the NMR hit. However, a wiser approach, based on NMR dynamic range considerations, is to search for and test for molecules structurally very similar to the original NMR hit but with superior solubility. This increases the possibility for the detection of the chemical scaffold with other biophysical techniques and most notably for the 3D structure determination of the scaffold bound to the receptor by X-ray or NMR.

The possibility of working at very low fragment concentration permits the testing of the fragments in large mixtures, thus enabling high-throughput NMR screening. This is particularly the case with the screening of mixtures of fluorinated molecules. A simulation of the behavior of p_b as a function of protein concentration $[E_T]$ for two binding constants K_D, 200 μM and 1 mM, and for two different fragment concentrations $[L_T]$, 20 and 200 μM, is reported in Figure 4. It is evident, according to the simulations of Figures 3 and 4 that the best sensitivity is reached by working at a low fragment concentration and a higher protein concentration. However, due to the large dynamic range, especially found in the ^{19}F R_2-filter experiments, the detection of fragments is possible even in the experimental conditions with a very small value of p_b. ^{19}F R_2 filter NMR screening has probably the largest dynamic range $[(R_b + R_{ex}) - R_f]$, and the theoretical explanation of this effect, which derives from several contributions, has been discussed in detail in two recent papers [47,49]. Therefore, it is possible to work at a low protein concentration, meaning a small protein consumption for the screening. Two experimental proofs of this were the detection of a fragment binding to human serum albumin and a fragment binding to trypsin through ^{19}F R_2-filter experiments in assays in which the p_b value for the two fragments was respectively only 0.00165 and 0.000563. This corresponds to one molecule bound and respectively 605 and 1775 free molecules [50,51].

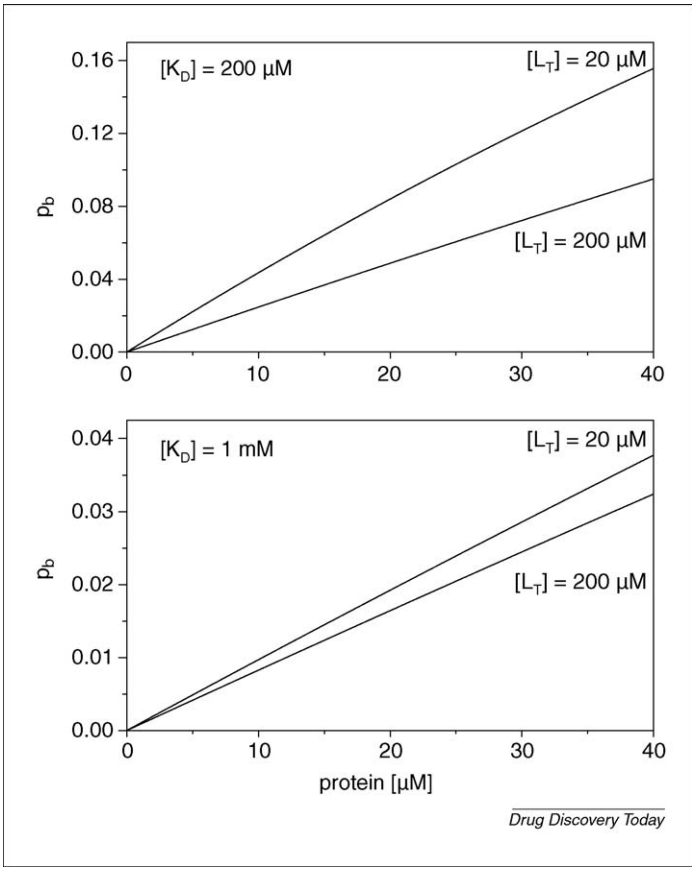

FIGURE 4

Simulation performed with Eq. (10) showing the fraction of protein-bound fragment p_b as a function of the protein concentration and for two different concentrations $[L_T]$ of the fragment as indicated on the graph. The simulations were performed with a fragment K_D of 1 mM (lower graph) and 200 μM (upper graph).

Ligand fluorine chemical shift perturbation

In addition to the R_2 parameter, ^{19}F-based screening experiments can use, in some favorable cases, the $\Delta_{obs} = (\delta_{obs} - \delta_f)$ observable parameter, where the terms δ_f and δ_{obs} are the fragment ^{19}F resonance chemical shifts in the absence and presence of the protein, respectively. For a very weak-affinity fragment (K_D in the mM range), the expression for Δ_{obs} is given by Eq. (11) [49]:

$$\Delta_{obs} \approx p_b \Delta_{max} \quad (11)$$

where $\Delta_{max} = (\delta_b - \delta_f)$ and δ_b is the chemical shift of the fragment ^{19}F resonance in the bound state. ^{19}F Δ_{max} can be very large thus allowing, in these favorable cases, the detection of very weak-affinity fragments through differences in chemical shift, as shown in the simulation of Figure 12 contained in Ref. [49].

Concluding remarks

It is fair to conclude that, according to the analysis reported here, NMR-based screening – despite having the lowest intrinsic

sensitivity – has the largest dynamic range (in particular, the ^{19}F monitored NMR experiments), enabling the detection of very weak interactions. However, it is also evident that NMR alone cannot provide the high-content information required in an FBDD process. Several biophysical techniques should be applied simultaneously and the data judiciously analyzed on the basis of the strengths, limits, possible pitfalls and complementarities of the various methods. This critical assessment is crucial for the identification of chemical scaffolds that have high potential for generating new therapeutic agents.

References

1 Macarron, R. (2006) Critical review of the role of HTS in drug discovery. *Drug Discov. Today* 11, 277–279
2 Hajduk, P.J. and Greer, J. (2007) A decade of fragment-based drug design: strategic advances and lessons learned. *Nat. Rev. Drug Discov.* 6, 211–219
3 Congreve, M. *et al.* (2008) Recent developments in fragment-based drug discovery. *J. Med. Chem.* 51, 3661–3680
4 Bartoli, S. *et al.* (2006) The fragment-approach: an update. *Drug Discov. Today: Technol.* 3, 425–431
5 Jahnke, W. and Erlanson, D.A., eds) (2006) *Fragment-Based Approaches in Drug Discovery*, Wiley-VCH
6 Jhoti, H. and Leach, A.R., eds) (2007) *Structure-based Drug Discovery*, Springer
7 Zartler, E.R. and Shapiro, M.J., eds) (2008) *Fragment-Based Drug Discovery*, John Wiley & Sons, Ltd.
8 Kahmann, J. *et al.* (2008) The impact of physical based method s screening and their delivery of better quality hits. *Drug Discov. Today: Technol.* 5, e15–e22
9 Hann, M.M. *et al.* (2001) Molecular complexity and its impact on the probability of finding leads for drug discovery. *J. Chem. Inf. Comput. Sci.* 41, 856–864
10 Siegal, G. *et al.* (2007) Integration of fragment screening and library design. *Drug Discov. Today* 12, 1032–1039
11 Kuntz, I.D. *et al.* (1999) The maximal affinity of ligands. *Proc. Natl. Acad. Sci. U.S.A.* 96, 9997–10002
12 Hopkins, A.L. *et al.* (2004) Ligand efficiency: a useful metric for lead selection. *Drug Discov. Today* 9, 430–431
13 Abad-Zapatero, C. and Metz, J.T. (2005) Ligand efficiency indices as guideposts for drug discovery. *Drug Discov. Today* 10, 464–469
14 Hajduk, P.J. (2006) Fragment-based drug design: how big is too big? *J. Med. Chem.* 49, 6972–6976
15 Cooper, M.A. (2002) Optical biosensors in drug discovery. *Nat. Rev. Drug Discov.* 1, 515–528
16 Englebienne, P. *et al.* (2003) Surface plasmon resonance: principles, methods and applications in biomedical sciences. *Spectroscopy* 17, 255–273
17 Papalia, G.A. *et al.* (2006) Comparative analysis of 10 small molecules binding to carbonic anhydrate II by different investigators using Biacore technology. *Anal. Biochem.* 359, 94–105
18 Hämäläinen, M.D. *et al.* (2008) Label-free primary screening and affinity ranking of fragment libraries using parallel analysis of protein panels. *J. Biomol. Screen.* 13, 202–209
19 Perspicace, S. *et al.* (2009) Fragment-based screening using surface plasmon resonance technology. *J. Biomol. Screen.* 14, 337–348
20 Navratilova, I. *et al.* (2007) Thermodynamic benchmark study using Biacore technology. *Anal. Biochem.* 364, 67–77
21 Markgren, P-O. *et al.* (2002) Relationships between structure and interaction kinetics for HIV-1 protease inhibitors. *J. Med. Chem.* 45, 5430–5439
22 Pope, A.J. *et al.* (1999) Homogeneous fluorescence readouts for miniaturized high-throughput screening: theory and practice. *Drug Discov. Today* 4, 350–362
23 Eggeling, C. *et al.* (2003) Highly sensitive fluorescence detection technology currently available for HTS. *Drug Discov. Today* 8, 632–641
24 Owicki, J.C. (2000) Fluorescence polarization and anisotropy in high throughput screening: perspectives and primer. *J. Biomol. Screen.* 5, 297–306
25 Valeur, B. (2001) *Molecular Fluorescence: Principles and Applications*. Wiley-VCH Verlag GmbH
26 Turconi, S. *et al.* (2001) Real experiences of uHTS: a prototypic 1536-well fluorescence anisotropy-based uHTS screen and application of well-level quality control procedures. *J. Biomol. Screen.* 6, 275–290
27 Turek-Etienne, T.C. *et al.* (2003) Evaluation of fluorescent compound interference in 4 fluorescence polarization assays: 2 kinases, 1 protease, and 1 phosphatase. *J. Biomol. Screen.* 8, 176–184
28 Gribbon, P. and Sewing, A. (2003) Fluorescence readouts in HTS: no gain without pain? *Drug Discov. Today* 8, 1035–1043
29 Turconi, S. *et al.* (2001) Developments in fluorescence lifetime-based analysis for ultra-HTS. *Drug Discov. Today* 6, S27–S39
30 Hoefelschweiger, B.K. *et al.* (2005) Screening scheme based on measurement of fluorescence lifetime in the nanosecond domain. *J. Biomol. Screen.* 10, 687–694
31 Moger, J. *et al.* (2006) The application of fluorescence lifetime readouts in high-throughput screening. *J. Biomol. Screen.* 11, 765–772
32 Jahnke, W. (2007) Perspective of biomolecular NMR in drug discovery: the blessing and curse of versatility. *J. Biomol. NMR* 39, 87–90
33 Pellecchia, M. *et al.* (2008) Perspectives on NMR in drug discovery: a technique comes of age. *Nat. Rev. Drug Discov.* 7, 738–745
34 Shuker, S.B. *et al.* (1996) Discovering high-affinity ligands for proteins: SAR by NMR. *Science* 274, 1531–1534
35 Hajduk, P.J. *et al.* (1997) Drug design—discovering high-affinity ligands for proteins. *Science* 278, 497–499
36 Morton, C.J. *et al.* (1996) Solution structure and peptide binding of the SH3 domain from human Fyn. *Structure* 4, 705–714
37 Fielding, L. (2007) NMR methods for the determination of protein–ligand dissociation constants. *Prog. Nucl. Magn. Reson. Spectrosc.* 51, 219–242
38 Dalvit, C. *et al.* (2000) Identification of compounds with binding affinity to proteins via magnetization transfer from bulk water. *J. Biomol. NMR* 18, 65–68
39 Mayer, M. and Meyer, B. (1999) Characterization of ligand binding by saturation transfer difference NMR spectroscopy. *Angew. Chem. Int. Ed.* 38, 1784–1788
40 Meyer, B. and Peters, T. (2003) NMR spectroscopy techniques for screening and identifying ligand binding to protein receptors. *Angew. Chem. Int. Ed.* 42, 864–890
41 Geschwindner, S. *et al.* (2007) Discovery of a novel warhead against β-secretase through fragment-based lead generation. *J. Med. Chem.* 50, 5903–5911
42 Edwards, P.D. *et al.* (2007) Discovery of novel cyclic amidine-based β-secretase inhibitors with nanomolar potency, cellular activity and high ligand efficiency. *J. Med. Chem.* 50, 5912–5925
43 Gossert, A.D. *et al.* (2009) Time efficient detection of protein–ligand interactions with the polarization optimized PO WaterLOGSY NMR experiment. *J. Biomol. NMR* 43, 211–217
44 Hajduk, P.J. *et al.* (1999) NMR-based screening in drug discovery. *Q. Rev. Biophys.* 32, 211–240
45 Salvatella, X. and Giralt, E. (2003) NMR-based methods and strategies for drug discovery. *Chem. Soc. Rev.* 32, 365–372
46 Peng, J.W. *et al.* (2004) NMR experiments for lead generation in drug discovery. *Prog. Nucl. Magn. Reson. Spectrosc.* 44, 225–256
47 Dalvit, C. (2007) Ligand- and substrate-based ^{19}F NMR screening: principles and applications to drug discovery. *Prog. Nucl. Magn. Reson. Spectrosc.* 51, 243–271
48 Manzenrieder, F. *et al.* (2008) Phosphorus NMR spectroscopy as a versatile tool for compound library screening. *Angew. Chem. Int. Ed.* 47, 2608–2611
49 Dalvit, C. (2008) Theoretical analysis of the competition ligand-based NMR experiments and selected applications to fragment screening and binding constant measurements. *Conc. Magn. Reson. Part A* 32A, 341–372
50 Dalvit, C. *et al.* (2003) Fluorine–NMR experiments for high-throughput screening: theoretical aspects, practical considerations, and range of applicability. *J. Am. Chem. Soc.* 125, 7696–7703
51 Vulpetti, A. *et al.* (2009) Design and NMR-based screening of LEF, a library of chemical fragments with different Local Environment of Fluorine. *J. Am. Chem. Soc.* 131, 12949–12959